

# Analysis of the effectiveness of repairing cracked aircraft structures: patch-performance criteria interaction

Imene Lariche, Mehadjia Bezzerrouki\*, Mohammed Amine Bellali,  
Mohammed Baghdadi, Boualem Serier

*LMPM Laboratory, Djillali Liabes University, Sidi Bel Abbes, Algeria BP 89,  
Cité Ben M'hidi, 22000 Sidi Bel Abbes, Algeria*

*(Received August 14, 2024, Revised September 10, 2025, Accepted October 31, 2025)*

**Abstract.** If hot bonding of the composite patch to the cracked plate leads to an improvement in the adhesion energy between these two protagonists, it is a source of residual stresses in the plate, the adhesive and the patch near their interfaces. Using FEM, this study aims to improve the performance of hot plate-patch joining and patch-crack interactions by optimizing the patch shape. Thus, all the patch shapes developed in this study arise from an initially rectangular shape. This results in six patch shapes: elliptical, orthogonal, star, H, double arrow and butterfly. This optimization is analyzed in terms of improvement in both the fracture energy gain of the plate (stabilization of the SIF with the evolution of the crack size  $\Delta K$ ), the mechanical energy gain of the adhesive (reduction of the risk of rupture of the adhesive by a drop in the level of shear stresses in the adhesive  $\Delta\tau$ ) and of the mass gain of the patch  $\Delta m$  (reduction of the risk of peeling and delamination and of debonding by an improvement of the aerodynamic resistance of the patch). These three gains,  $\Delta K$ ,  $\Delta\tau$ ,  $\Delta m$ , developed for the first time in this study, constitute characteristic criteria for the performance of composite patch repair. This is where the originality of this work lies. This study highlights that improving the fracture energy gain alone is not a sufficient condition for the effectiveness of hot repair. Thus, the simultaneous satisfaction of these three criteria is a necessary condition for the durability and performance of the repair. This therefore constitutes the originality of this study which lies in the development of these criteria. It appears from this study that the repair using an optimized double arrow-shaped patch leads to the satisfaction of these criteria. This shape simultaneously ensures stabilization of the three components of the repair: the plate by stabilizing the crack, the adhesive by reducing shear stresses, the patch by reducing its mass. The risks of damage (debonding, peeling, delamination) due to these stresses and the size and thickness of the patch are clearly minimized. It also emerges from this study that, contrary to previous works, hot bondings of the patch to the cracked plate doesn't in any way affect the performance of the hot repair using an optimized patch.

**Keywords:** adhesive; composite patch; crack; energy gain; hot adhesion; interaction; mass gain; performance criteria; rigidity; shear; stress; wettability

---

## 1. Introduction

Discontinuity defects such as cracks, holes, notches, cavities, surface irregularities etc. may arise during the materials commissioning process. These imperfections constitute a source of damage to these materials responsible for the degradation of their in-service performance and their

---

\*Corresponding author, Professor, E-mail: [m.bezzerrouki@gmail.com](mailto:m.bezzerrouki@gmail.com)

rigidity [1]. To overcome this problem and to restore these two mechanical characteristics, it is strictly necessary to repair the areas of damage using a bonded composite patch. This repair technique, initially used in the field of aeronautics and aerospace, has been extended to other areas of industry particularly in maritime engineering, civil engineering, renewable energy (repair of wind turbines). Thus, the presence of the composite patch makes it possible to relax the highly localized stress concentrations in the damage zone, which makes it possible to stabilize the weakened zone of the structure. If this zone is damaged by cracking, the patch leads to a stabilization of the crack propagation kinetics by a strong reduction in the stress intensity factor (SIF). This behavior results in an improvement in the durability of the initially cracked structure [2-5]. Optimizing the shape of the patch remains one of the necessary means for reducing the SIF at repaired crack tips [6, 7]. This reduction is closely linked to the capacity of load transfer from the crack front to the composite patch through the adhesive joint. In this repair technique, the patch can be cold or hot bonded to the cracked area. It should be noted that if hot bonding leads to an improvement in the adhesion energy between these two protagonists by good spreading of the adhesive on the cracked substrate, it is a source of additional residual stresses which can lead to instability of the repaired crack. It should be noted that very few studies have been devoted to the behavior of cracked and hot-repaired structures. Thus, a study of Deheeger et al. [8] relating to the evaluation of the distribution of thermal stresses in the bonding of the composite to aluminum, shows that a peak of shear stress occurs in the adhesive near the free edge of the patch. In the same context, work of Azzouz et al. [9] illustrates that hot repair by composite patch of cracked aircraft structures generates an average increase in SIF of approximately 40%, and 60% at long crack front. In this same context, it was demonstrated that the hot bonding of the patch to the cracked zone of the aircraft plates induces, in these two materials, residual stresses responsible for the increase in the stress intensity factor in mode I [10]. In the same sense, the residual stresses induced in the adhesive and the plate near the interface during a hot repair increase the instability of the repaired crack compared to a cold repair [11]. Other studies have demonstrated that the existence of residual stresses of thermal origin induced during hot repair considerably reduces the performance of the repair from the point of view of reduction of the stress intensity factor in mode I [11-13]. For these reasons and until now, cold repair is predominant. The performance of this repair technique was essentially analyzed in terms of reduction of the stress intensity factor "SIF" at the repaired crack tips [14-21].

Contrary to what has been predicted so far, this work aims to contribute, numerically through MEF, to improving the performance of hot repair by bonded composite patch of aircraft structures through a parametric optimization of a patch shape allowing both stabilization of the hot repaired crack of the Al2024T3 plate, the adhesive joint and the composite patch, by a simultaneous reduction of the SIF, the level of shear stresses and the mass of the patch respectively. These three physical parameters, developed for the first time in this study are denoted  $\Delta K$ ,  $\Delta\tau$  and  $\Delta m$ , constitute performance criteria for the bonded composite patch repair. This study highlights that the effectiveness of the repair is closely simultaneously linked to the stability of the plate by gain in fracture energy at the repaired crack fronts ( $+\Delta K$ ), to the stability of the adhesive by a gain of mechanical energy ( $+\Delta\tau$ ) and the stability of the patch by a mass gain ( $+\Delta m$ ). It should be noted that practically all the work devoted to patch repair has been based on improving the performance of the repair in terms of reducing the fracture energy at the tip of the repaired crack, in particular the stress intensity factor.

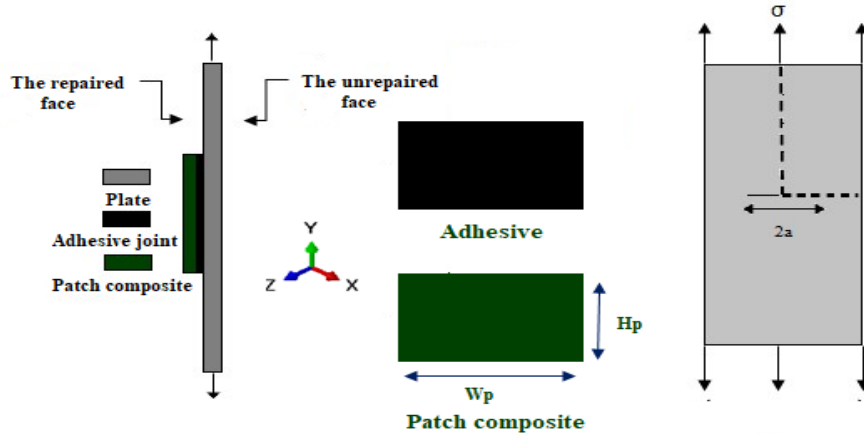


Figure 1. Cracked plate repaired by hot bonding patch

Table 1. Mechanical properties of the structure elements [22, 23]

E et G [GPa]	$E_1$	$E_2$	$E_3$	$G_{12}$	$G_{13}$	$G_{23}$	$\nu_{12}$	$\nu_{13}$	$\nu_{23}$	$\alpha(10^{-6}\text{C}^{-1})$
Plate Al (2024-T3)	72						0.33			22.5
Patch (Carbon /epoxy)	153	9.1	9.1	4.57	4.57	3.15	0.258	0.258	0.384	4.5
Adhesive (FM73)	2.55			0.42			0.3			0.21

## 2. Numerical model

The developed model consists of a rectangular plate in 2024T3 aluminum alloy, with dimensions: 250x125x2 mm, containing a central rectilinear crack of size  $2a$ , located along the transverse direction of the plate. The latter, requested in pure mode I, was repaired using a carbon/epoxy patch, initially rectangular with height  $H_p = 40$  mm, width  $W_p = 80$  mm and thickness  $e_p = 2$  mm. These parameters have been optimized for the repair of a 28 mm crack (Fig. 1). The patch was bonded to the cracked area at a temperature of  $100^\circ\text{C}$ . Thus, the plate-patch interface is assumed to be perfectly bonded to the plate using an FM-73 adhesive, thickness  $e_a = 0.2$  mm (Fig. 1) and properties at Table 1 which is a characteristic of hot bonding of the patch to the plate.

The shear strength ( $\tau_r$ ) of the FM73 adhesive at  $T=20^\circ\text{C}$  is  $\tau_r = 35$  to  $45$  MPa. It should be noted that the toughness of the Al 2024 T3 plate at room temperature is  $23 \text{ MPa}\cdot\text{m}^{1/2}$ . The mechanical strength of the 2024T3 alloy practically doesn't decrease up to a temperature of  $150^\circ\text{C}$  [23].

### 2.1 Modeling by finite element method

The finite element method was used for prediction of the performance of hot bonded composite patch repair. Modeling by this method requires the meshing of the structure, composed of the cracked plate, the adhesive joint and the patch. The choice of the types and sizes of elements to use, particularly at the crack tip, depends on the fundamental parameters, to control the strong stress and strain gradients in the vicinity of the crack tip. Thus, the first step consists of choosing

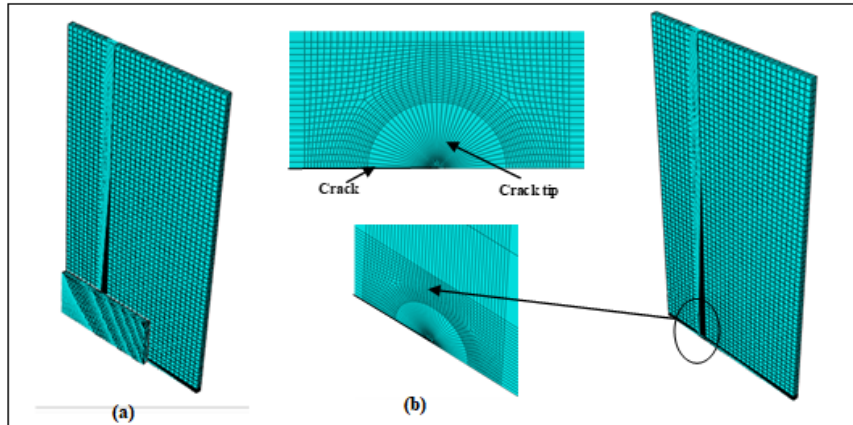


Figure 2. Mesh of the analyzed structure

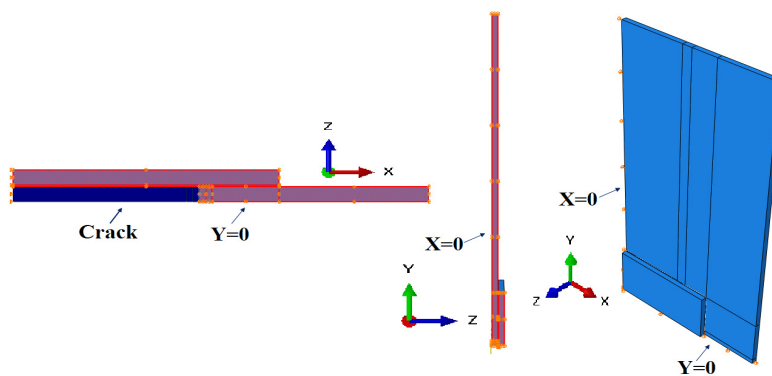


Figure 3. Boundary conditions imposed on the plate/adhesive/patch assembly

Table 2. Number of elements per constituent of the structure

The different components of the structure	Numbers of elements	Sizes of elements (mm)
Plaque AL2024T3	11796	2
Crack front	2080	0.078
Patch	3200	0.5
Adhesive FM73	800	1

the type of element, the most suitable for the problem studied, then the structure is divided into a certain number of elements. In accordance with fracture mechanics and finite element modeling of a cracked plate, the structure was globally meshed using C3D8 type elements (A linear brick with 8 nodes) (Fig. 2). The total number of elements for the repaired structure depends on the shape of the patch. For a rectangular geometry, the total number of elements is illustrated in Table 2. The mesh was exceptionally refined near the cracking defect, particularly in the very close vicinity of the crack fronts, using Barsoum elements [24] (Fig. 2). Due to its high symmetry, only a quarter of

the structure was taken into consideration in this analysis (Fig. 2). The boundary conditions imposed on this structure are clearly indicated in Fig. 3.

These simulation conditions will be maintained throughout this study. The elastic approach was chosen for this study. This approach was deliberately chosen in order to analyze the performance of the repair, in terms of high stress and extremely long crack sizes, under the most extreme mechanical conditions.

### 3. Adhesion plate-patch for a hot repair

#### 3.1 Adhesion energy

Very few studies have been devoted to hot bonding of the patch to the damage zone of aircraft structures. It has been clearly defined that the mechanical strength in service of the plate-patch interface is closely linked to the wettability of the plate by the FM73 adhesive (Fig. 4). Thus, the spreading of the liquid adhesive is ideal when the wetting angle  $\theta$  tends towards a zero value, in this case the surface of the Al2024T3 plate is ideally covered with a film of thin liquid adhesive.

This phenomenon leads to the fundamental equation of adhesion known as Dupré [1], or the adhesion energy.

The latter is closely linked to the contact angle plate-FM73 adhesive by Hattali [25]

$$W_a = \gamma_L(1 + \cos\theta), \quad (1)$$

This relationship shows that the maximum value of the adhesion energy of all the liquid wetting a surface is  $2 \gamma_L$ , for an ideal spreading  $\theta=0^\circ$ , independently of the solid in contact. It is established that the surface energy depends on the temperature, it increases when the temperature drops [26]. The viscosity of the adhesive, a fundamental spreading parameter, drops with increasing temperature and leads to good wettability. In this case, the adhesive tends to minimize the contact angle with the aluminum alloy plate on the one hand, and with the patch on the other hand. This minimization leads to an increase in adhesion energy, characteristic of intimate contact at the plate-patch interface. This phenomenon improves load transfer from the cracked area of the plate to the composite patch and minimizes the risk of peeling, delamination and debonds of the patch from the cracked plate. This constitutes a necessary condition to make the performance of the repair profitable in terms of fracture energy gain at the repaired crack tips. The improvement of this transfer is simulated in this study by a perfectly bonded plate-patch interface. If hot bonding of the patch to the cracked plate has such an advantage, it is a source of residual stresses. Do these affect the performance of the repair? This study provides an explicit answer to this question.

#### 3.2 Residual stresses

It is well established that this type of adhesion generates residual stresses in the plate, the adhesive and in the patch in the vicinity of their interface. These stresses develop due to the difference between the thermal expansion coefficients of the plate and that of the adhesive joint, on the one hand, and the gap between the latter and that of the patch, on the other hand. The thermal deformations of these two interfaces denoted respectively (I) and (II), unrelated are obtained [26]

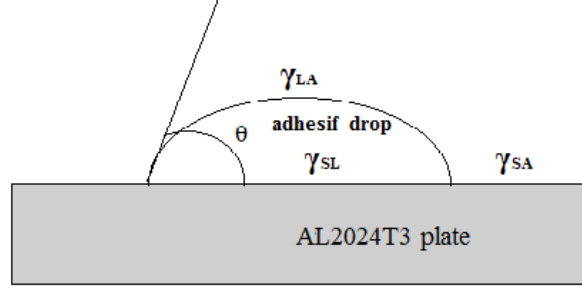


Figure 4. Mechanism for wetting the cracked plate with liquid adhesive [23]

$$\text{At the interface I: } (\varepsilon_{pl})_I = \alpha_{pl} (T - T_0)_I \text{ and } (\varepsilon_{ad})_I = \alpha_{ad} (T - T_0)_I, \quad (2)$$

$$\text{At the interface II: } (\varepsilon_{ad})_{II} = \alpha_{ad} (T - T_0)_{II} \text{ and } (\varepsilon_{pa})_{II} = \alpha_{pa} (T - T_0)_{II}. \quad (3)$$

Interface I: between the cracked plate and the adhesive, and interface II: between the adhesive and the composite patch. We are exclusively interested in interface I cracked plate-adhesive whose  $\Delta\alpha = (\alpha_{pl} - \alpha_{ad})$  is ten times greater than that of interface II (Table 1).

$\varepsilon_{pl}$ ,  $\varepsilon_{ad}$ ,  $\varepsilon_{pa}$  are the deformations of the cracked plate, the adhesive layer and the composite patch respectively,  $(\varepsilon_R)_I$ ,  $(\varepsilon_R)_{II}$  the thermal residual deformations at interfaces I and II respectively and  $\alpha_{pl}$ ,  $\alpha_{ad}$ ,  $\alpha_{pa}$  of thermal expansion coefficients of the respective cracked plate, adhesive layer and composite patch.

The differences between the temperature at which the patch is bonding to the cracked area of the plate and the reference temperature are:  $\Delta T_I = (T - T_0)_I$  and  $\Delta T_{II} = (T - T_0)_{II}$

### 3.2.1 Rectangular patch-crack interaction

Bonding the plate to the patch leads to the equalization of the deformations  $(\varepsilon_{pl})_I$  and  $(\varepsilon_{ad})_I$ , at interface I, on the one hand, and  $(\varepsilon_{ad})_{II}$  and  $(\varepsilon_{pa})_{II}$  at interface II of on the other hand, which leads to residual deformations at interface I  $(\varepsilon_R)_I$  and at interface II  $(\varepsilon_R)_{II}$  with which residual stresses are associated. Depending on the physical coefficient of linear thermal expansion “ $\alpha$ ”, these stresses put, near the interface I; the plate in tension and the adhesive joint in compression, and in the close vicinity of interface II, the adhesive in compression and the patch in tension. This behavior generates an auxiliary bending moment in the repaired plate, which stresses the patch near interface II in compression and in the vicinity of its non-bonded face in tension. Due to its high stiffness, the patch induces a buckling of the repaired structure along the Y direction of the plate/adhesive/patch assembly (Fig. 5). The internal stresses resulting from this phenomenon act as crack opening forces. This explains the relatively high values of the mode I rupture energy (SIF) obtained.

It should be noted that the composite patch is the most rigid link in the plate/adhesive/patch chain. To this end, this study is particularly interested in the cracked zone interface of the plate-adhesive joint, denoted interface I, while taking into account the interaction of the adhesive joint-patch interface, denoted interface II. The mode I behavior of the crack is controlled by the residual tensile stresses strongly localized at the cracking fronts of the plate near the interface I. These stresses act on the crack as opening forces and are responsible for the propagation of the crack. To

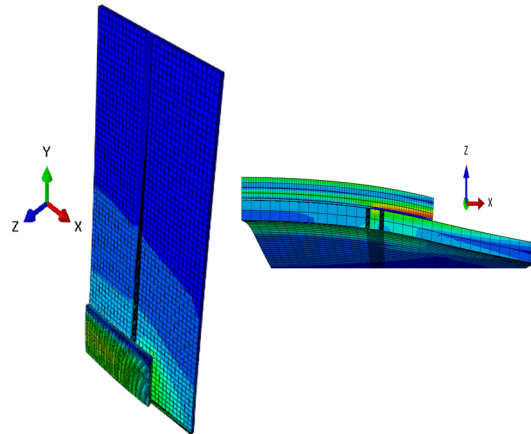


Figure 5. Effect of the patch on the buckling of the cracked plate of the thermally produced plate/adhesive/patch assembly

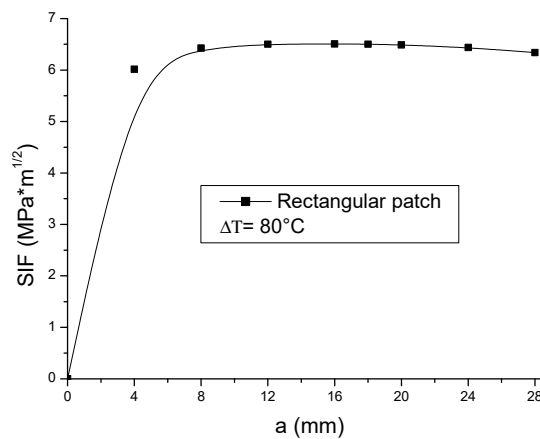


Figure 6. Patch-stability interaction of SIF in hot-repaired crack tips

this end, the presence of the patch ensures the delay of the propagation kinetics by a phenomenon of stabilization of the (SIF), due to the presence of normal residual tension stresses developed in the cracked plate near the interface with the joint of adhesive regardless of the size of the repaired crack and shows that this rupture parameter varies asymptotically with the evolution of the crack (Fig. 6). This leads to an improvement in the service life of the hot repair.

The normal residual stresses of compression in the adhesive joint and tension in the cracked plate generate at interface I shear stresses specific to the YOZ, XOY and XOZ planes of the plate/adhesive/patch assembly (Fig. 7). These stresses, analyzed in the adhesive joint, upstream of the crack front at the free edge with the patch. Compared to the stresses induced in the last two planes, those generated in the first plane are the most significant. Only these stresses, placing greater demands on the adhesive, will be taken into consideration in the remainder of this study.

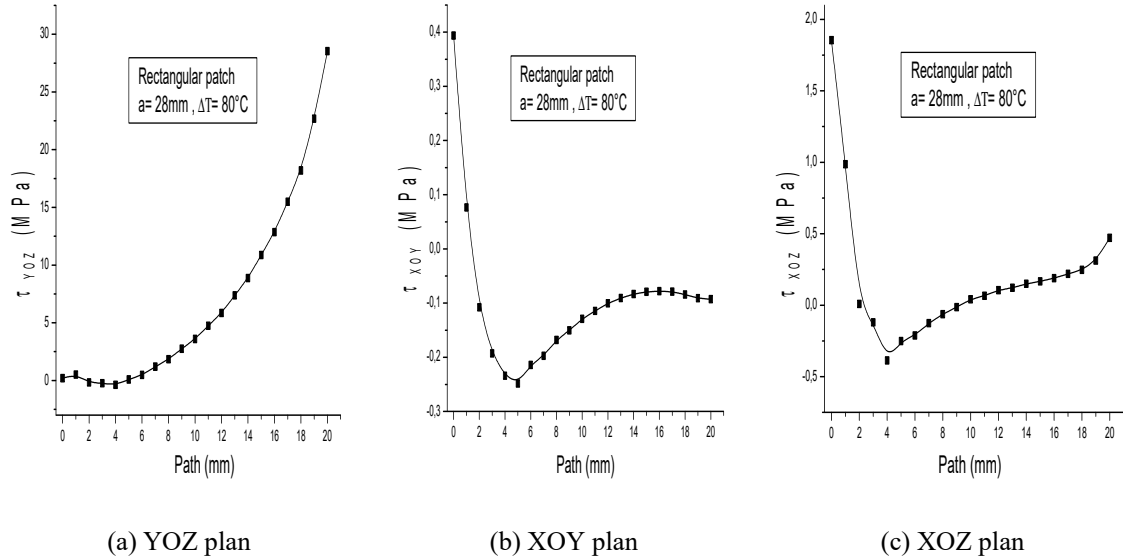


Figure 7. Level of internal tangential stresses in the adhesive at interface I

Remember that the FM 73 adhesive has low mechanical resistance to shear [27] and therefore relaxing the adhesive from these stresses is a necessary condition for improving the performance of the repair in terms of service life and fatigue life of this assembly. These two physical parameters (Fig. 6 and Fig. 7), the rupture energy and the shear stresses, are significantly linked to the effectiveness of the patch [28-34].

### 3.2.2 Patch shape-crack interaction

Contrary to the most of the works carried out to date based on the rupture energy gain in mode I (stability of the SIF) as a repair performance criterion, this study fails to develop the characteristic criteria of the performance of the repair linked to its three components plate-adhesive-patch. In other words, it aims to stabilize these three components of the repair by a simultaneous reduction of the fracture energy at crack front of the plate, shear stresses in the adhesive, and the mass of the patch. Physically relieving these components during the commissioning process of the hot plate-adhesive-patch assembly, makes a significant contribution to improving the effectiveness of the repair. This reduction can only be achieved by optimizing the patch shape from its initially rectangular shape (Fig. 8). Thus, all the patch shapes developed in this study arise from an initially rectangular shape. These results in six patch shapes: elliptical, orthogonal, star, H, double arrow and butterfly. Given the high symmetry of the geometry of these shapes, only their quarter was taken into consideration (Fig. 8). It should be noted that the developed patches are only distinguished by their shapes and their covering surfaces.

The repair modeling was carried out under the same simulation conditions as those used previously. The results obtained, illustrated in Fig. 9, clearly show that the effectiveness of the patch, in terms of relaxation of the residual tension stresses in the repaired cracked plate (stability of the SIF with the evolution of the size of the crack) is sensitive to the shape of the patch. It is explicitly indicated in this figure that the kinetics of mode I propagation of the crack is slowed

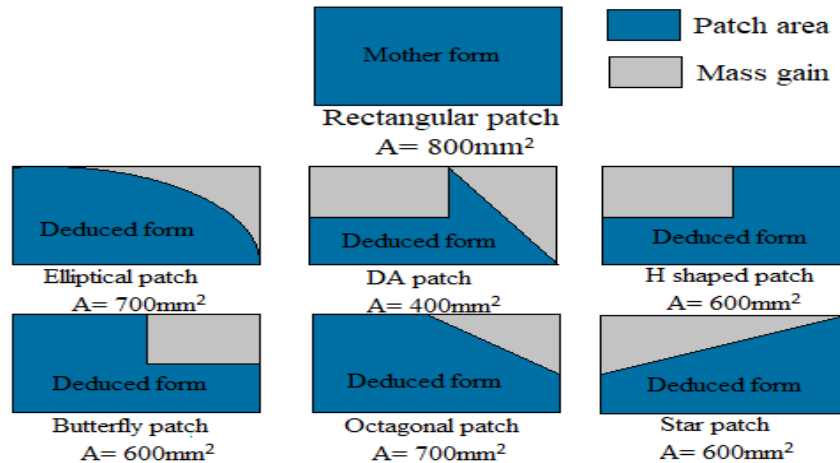


Figure 8. Developed patch shapes

down even more as the repair is carried out using a patch having a small covering surface and vice versa. Thus, the repair using a patch in the shape of a double arrow is significantly more efficient in terms of stability of the crack (gain in fracture energy SIF ( $+\Delta K$ )), and stability of the patch (gain in mass ( $+\Delta m$ )). Thus, the rectangular patch, twice as large in size, generates an opposite effect. From the five remaining patch shapes, having intermediate overlapping areas between the rectangular shape and the double arrow shape, an intermediate behavior results. Contrary to the rectangular patch, all other shapes have a significantly lower coverage volume, which leads to too much mass saving and makes the repair profitable from a cost and safety point of view. It should be noted that the plus (+) and minus (-) signs, used in this study, represent respectively the gain and the deficit in physical parameters linked to the three components of repair: plate ( $\Delta K$ ), adhesive ( $\Delta \tau$ ) and patch ( $\Delta m$ ).

The most significant shear stresses relating to the YOZ plane of the plate/adhesive/patch assembly, generated in the adhesive, are all the lower as the repair uses patches of reduced size (Fig. 10). For this purpose, the lowest level of these efforts is induced by a double arrow patch. It should therefore be noted that for such patches, the optimal performance of the repair, in terms of simultaneous gains in rupture energy ( $+\Delta k$ ) of the plate (Fig. 9), in shear stresses in the adhesive ( $+\Delta \tau$ ) (Fig. 10) and in mass of the patch ( $+\Delta m$ ) (Fig. 8), is obtained by a patch in the shape of a double arrow. In other words, the effectiveness of the repair, from a cost, safety and durability point of view, is closely linked to the satisfaction of these three physical parameters, developed in this study and defined here as characteristic performance criteria: Gain of propagation energy as a parameter characteristic of the stability of the damage of the plate, gain in tangential forces as a criterion for the stability of the adhesive and gain in mass as a parameter indicating the stability of the patch. Due to the existence of sharp sharp edges, the double arrow (DA) patch is likely to store a large quantity of the energy transferred from the crack fronts through the adhesive joint to the repair material. This phenomenon is at the origin of the stability of the growth in mode I of the repaired crack and is characterized by an asymptomatic variation of the SIF with the evolution of the size of the crack (Fig. 9). Contrary to the rectangular mother shape, repair using this type of patch leads to both a gain in fracture energy at repaired crack front ( $+\Delta K$ ), by a reduction in the SIF

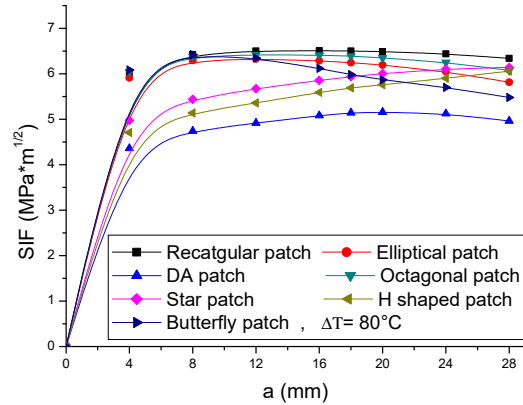


Figure 9. Interaction patch shape and fracture energy gain at crack tips

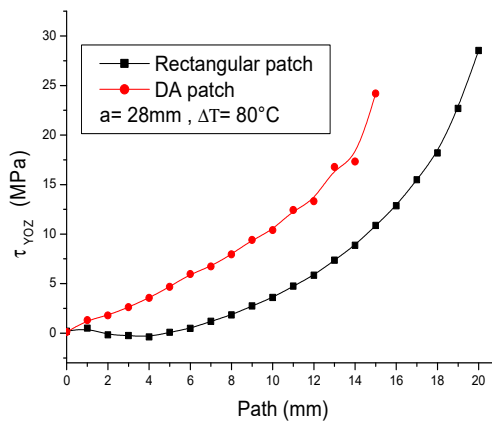


Figure 10. Interaction patch shape and gain in shear stress induced in the adhesive

and a gain of mechanical forces ( $+\Delta\tau$ ), by a more significant drop in shear stresses in the adhesive (Fig. 9 and Fig. 10). It should be noted that this double-arrow patch has a doubly smaller covering surface than the parent form (Fig. 8), this results in a gain in mass ( $+\Delta m$ ) doubly greater, which promotes efficiency and the stability of the composite patch and minimizes the physical phenomena that may be caused by the large size of the patch and more particularly its thickness. Indeed, such a size is generally responsible for plate buckling, peeling, delamination, aerodynamic resistance, repair and delamination. Thick patches favor such behavior and generally lead to the degradation of the plate-adhesive-patch chain through a phenomenon of decohesion of the patch from the cracked area of the plate. On the other hand and in accordance with the results illustrated from Fig. 8 to Fig. 10, compared to other patch geometries, the double arrow patch, having a more aesthetic shape, leads to better efficiency of the repair by a simultaneous reduction of the SIF in front crack of the plate, the level of shear stresses in the adhesive layer and the mass of the patch.

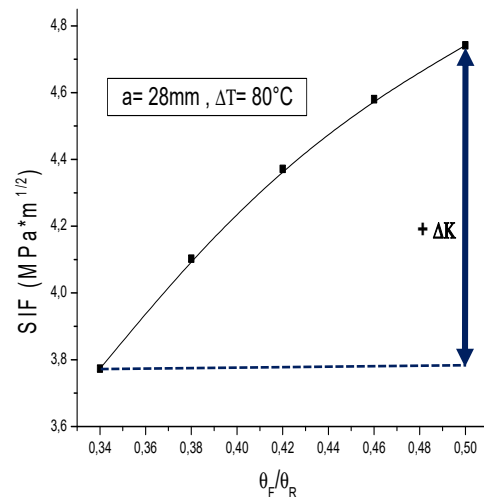
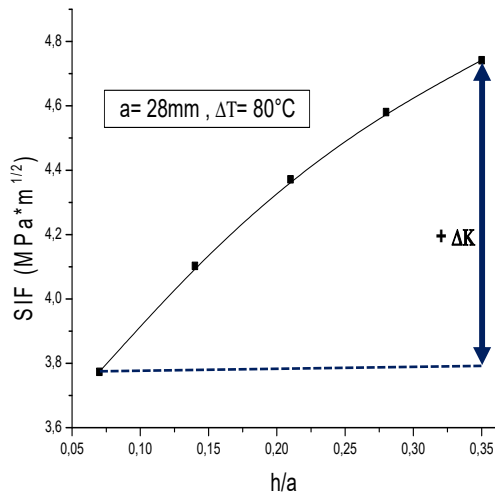
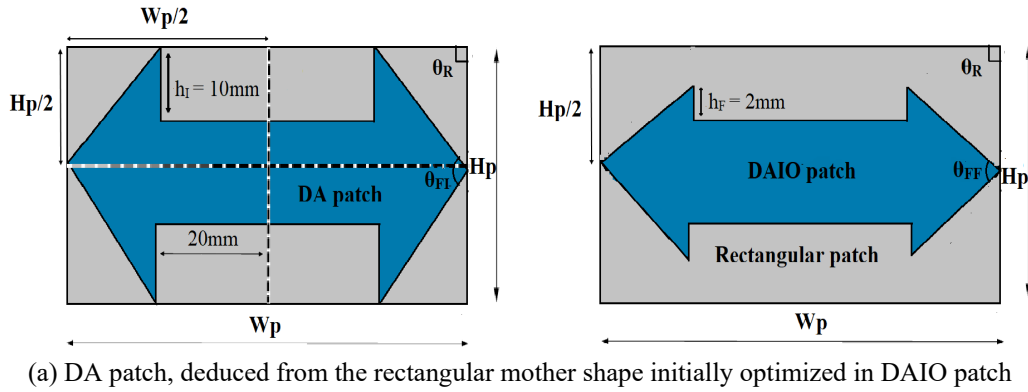
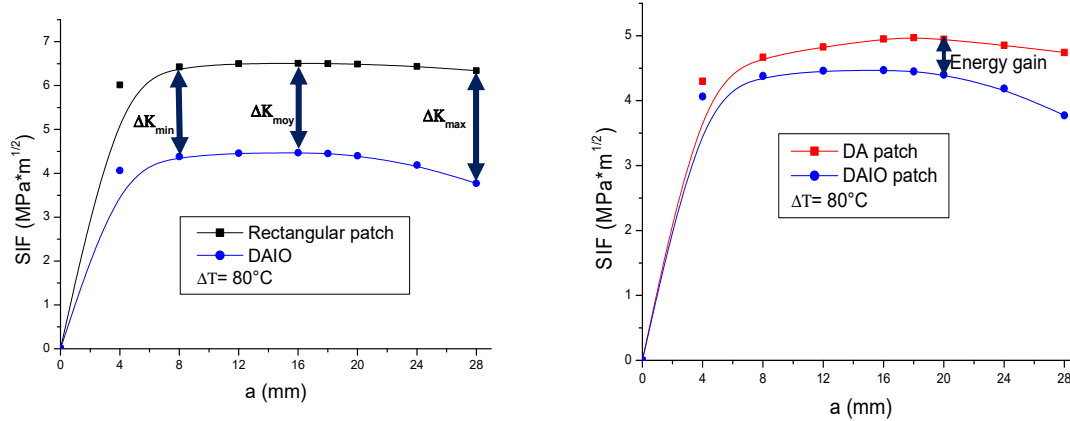


Figure 11. Effect of the dimensional parameters of the double arrow patch on the SIF at a crack tip repaired

### 3.2.3 Double arrow patch-crack interaction

The satisfaction of these three criteria, rupture energy gains ((+ΔK), mechanical energy gain (+Δτ), and mass gain (+Δm), is therefore necessary condition for improving the performance of repair. This can only be achieved by optimizing the dimensional parameters of this form of patch (Fig. 11). For this purpose, the width of the patch  $W_p$  is invariable, only the parameter  $H_p$  fluctuates. Thus, the magnitude “h” systematically generates a reduction in the angles denoted by  $\theta$  of the extreme parts of the patch double arrow (DA) (Fig. 11(a)). In other words, a reduction in the ratios “h/a” (h is the height of the arrow, « a » the size of the crack (Fig. 11(b)) and  $\theta_F / \theta_R$  (where  $\theta_F$  is the angle at the corner of the double arrow patch DA,  $\theta_R$  the angle at the corner of the rectangular patch (Fig. 11(c)), initially optimized, and denoted DAIO, explicitly leads to an improvement in the gain in breaking energy of the plate (+ΔK), in the gain of shear stress in the adhesive (+Δτ), and in the gain in mass (+Δm), by both a reduction in the SIF of the plate cracked,



(a) Interaction patch shape-SIF in mode I

(b) Interaction optimized patch shape -SIF in mode I

Figure 12. I interaction optimized patch shape- $\Delta K$  energy gain

a reduction in the shear stresses in the adhesive and a reduction in the mass of the patch. Compared to the DA patch, the initially optimized DAIO patch presents a mass gain of 20%, and a too significant mass gain of 70% ( $+\Delta m$ ) compared to the rectangular mother shape.

### 3.2.4 DAIO patch stiffness-crack interaction

The repair using an initially optimized double arrow patch, denoted DAIO, is significantly more efficient, in terms of satisfying the three criteria ( $+\Delta K$ ), ( $+\Delta\tau$ ), ( $+\Delta m$ ), developed previously, than those resulting from a double arrow patch, DA, (Fig. 12). The latter explicitly shows that the fracture energy, SIF, drops in intensity once the cracking front crosses the triangular overlap zone (arrows) of the extreme parts of the double arrow patch. In other words, the development of the crack from the rectangular central part of the DA patch towards the triangular external parts leads, with the advancement of the crack, to a regression of this rupture parameter (Fig. 12(a)). Thus, extremely long cracks with sizes greater than 20mm are significantly more stable, in terms of fracture energy values (SIF), than short cracks with sizes less than 20 mm. The latter delimits the rectangular zone from the triangular zone of the DA patch (Fig. 8). This behavior is closely linked, not only to the reduction of the residual tension stress field in the plate in contact with the triangular zone, with also to the minimization of the buckling effect of the plate in this part of the patch in contact with the cracked area of the plate (Fig. 5). These two combined phenomena, due to the reduction in the contact area between these two protagonists, are responsible for the fall in the SIF of the plate and the mass of the patch (Fig. 12(a)). On the other hand, contrary to a repair using a rectangular patch (Fig. 12(a)), where the SIF varies asymptotically with the propagation of the crack, in the case of a repair using a double arrow DA patch, the SIF is clearly more reduced. This phenomenon is due not only to the geometry of the patch, but also to the doubly smaller overlapping surface of the DA patches. The non-variation of the contact area of the rectangular patch, whatever the size of the repaired crack, leads to an asymptotic variation of the rupture energy, SIF (Fig. 12(a)). In the case of a DA patch and for long cracks (of sizes  $a > 20$  mm), the contact area decreases with the evolution of the size of the repaired crack, which explains the

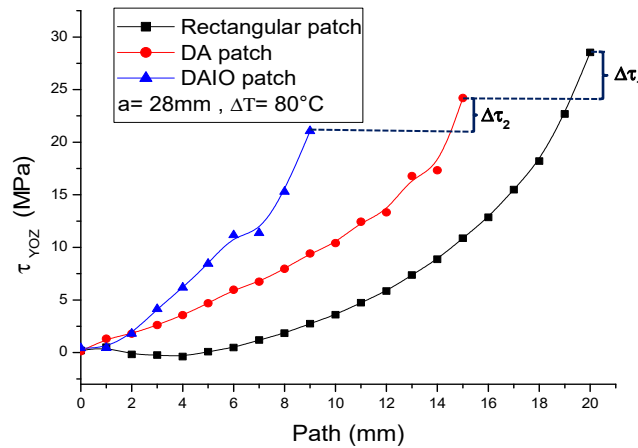


Figure 13. Interaction patch shape- gain shear stress ( $\Delta\tau$ ) in the adhesive

decrease in the SIF with the increase of the crack length (Fig. 12(a) and (b)). A more marked reduction in the contact area, in the case of the DAIO patch, leads to a more pronounced regression of the SIF with the growth of the crack (Fig. 12(b)). This reduction simultaneously generates internal tension stresses in the plate and in the adhesive of low intensity internal compressive stresses. These two forces place less shear stress on the adhesive interface (Fig. 13). Indeed, compared to a repair using a rectangular patch, the repair using a DA patch induces less intense shear stresses in the adhesive (Fig. 13).

These results show that, compared to the performance of the repair using a patch of rectangular mother geometry, the initially optimized double arrow patch shape “DAIO”, for the same size of repaired cracks «  $a=28$  mm », the propagation kinetics are explicitly more delayed, in terms of a strong reduction in SIF (Fig. 12(a)). Which is very interesting in terms of crack stability. It should be noted, however, that contrary to the DA patch, the optimized DAIO patch leads to a mass gain of around 20%, and compared to the rectangular mother shape a gain of 70% (Fig. 8). This greatly minimizes the risk of damage to the repair, through a phenomenon of peeling, delamination and debond, due to the large patch size and promotes improvement in fatigue life. This behavior explicitly illustrates that the repair using a DAIO patch is significantly more efficient, in terms of simultaneous gains in fracture energy ( $+\Delta K$ ) at crack tips, and shear force ( $+\Delta\tau$ ) in the adhesive and mass ( $+\Delta m$ ) of the composite patch. This ensures both plate damage stability, adhesive stability and composite patch stability respectively during the commissioning process.

It emerges from this analysis that compared to the double arrow patch (DA), the initially optimized double arrow patch (DAIO), leading simultaneously to a reduction or even a stop in the growth speed in mode I of the crack (stabilization of the SIF) to a reduction in the probability of rupture of the adhesive (drop in the level of shear stresses), and of lightening of the patch (reduction of mass), is significantly more effective (Fig. 9 and Fig. 10). The impact of these stresses on the mechanical behavior of the adhesive interface between the patch and the cracked plate is distinctly less significant. Thus, compared to the rectangular mother shape, the DAIO patch generates doubly less intense shear stresses in the adhesive (Fig. 13). This behavior strongly

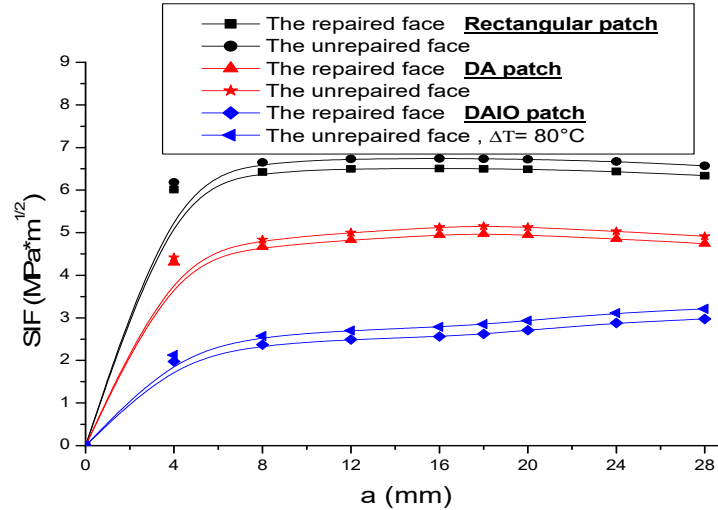


Figure 14. Interaction patches shape-energy gain of the repaired and unrepaired face

contributes to enhancing the performance of the repair through better service life of the adhesive. These stresses are often the cause of the degradation of cracked plate/adhesive/patch assemblies, because the damage to the adhesive interface results in a phenomenon of separation of the patch and accompanied by instability (propagation) of the crack of the plate [22]. To this end, reducing the level of these stresses is a necessary condition for the evolution of the effectiveness of the patch, in terms of improving the resistance to debond and the service life of the repair.

The stability, in terms of fracture energy gain “SIF”, of the crack on the repaired face is almost similar to that of the crack on the unrepaired face. The SIF values relating to these two faces are comparable regardless of the size of the repaired cracking defect (Fig. 14). This behavior explicitly illustrates the effectiveness of the patch along the thickness of the plate. In other words, the patch-face interaction of the unrepaired plate is as strong as that with the repaired face. This leads to an improvement in the service and fatigue life of the repaired plate and makes double bond repair unnecessary.

This study clearly illustrates that the stabilization of the stress intensity factor “SIF” with the evolution of the size of the repaired crack is not a sufficient condition for the assurance and prediction of the performance of the repair. The stabilization of the two other components of the structure, in this case the adhesive and the patch, by a drop in the level of shear stresses in the adhesive and the mass of the patch, is a necessity for obtaining an effective repair. Compared to all the forms studied, the repair using a DAIO patch, in terms of gain simultaneously in fracture energy of the plate (+ $\Delta K$ ), shear stress of the adhesive (+ $\Delta\tau$ ) and mass of the patch (+ $\Delta m$ ), is more profitable. These gains, developed in this study, now constitute repair performance criteria. It should be remembered that the two patches DA and DAIO, have the same thickness  $e_p=2$  mm, only differ in the covering area.

This study, based on a dimensional parametric optimization, from an initially rectangular shape, led to the development of a patch in the shape of a DAIO double arrow allowing the

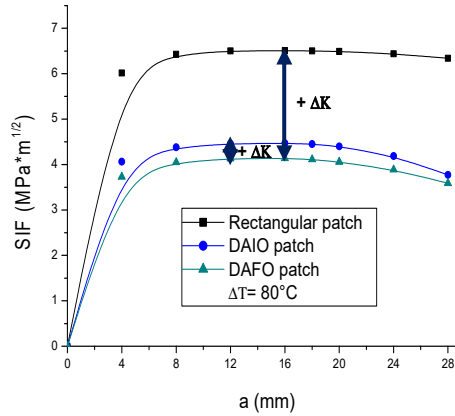


Figure 15. Interaction of optimized patch shape DAFO- rupture energy gain in plate (+ $\Delta K$ )

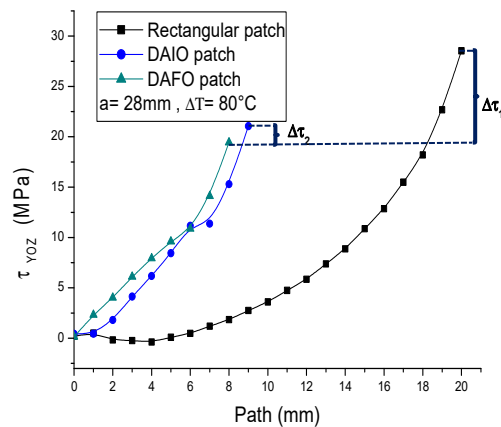


Figure 16. Interaction of optimized patch shape DAFO-Shear stress in the adhesive (+ $\Delta\tau$ )

satisfaction of these three criteria at the same time. Hot bonding using DAIO patch ( $ea=2$  mm), with a doubly reduced mass, twice as thin and denoted double arrow optimized final DAFO ( $ea=1$  mm), to the cracked plate leads to a reduction in the SIF (Fig. 15). This figure shows that compared to an initially optimized DAIO patch, a reduction in the rigidity of the patch leads to better stability of the repaired crack in terms of plate rupture energy gains (+ $\Delta K$ ) and mass gain (+ $\Delta m$ ). This behavior is observed regardless of the size of the crack. Indeed, this reduction minimizes the intensity of the compressive stresses generated by the buckling of the plate and due to the difference in stiffness between the plate and the patch. In addition to the residual tension stresses, these additional stresses resulting from this phenomenon act as crack opening forces. This explains the relatively low values of the mode I rupture energy (SIF) obtained compared to those induced by a doubly stiffer patch. Due to its low stiffness and compared to the DAIO patch, this type of DAFO patch induces low intensity shear stresses in the adhesive joint and leads to a gain in

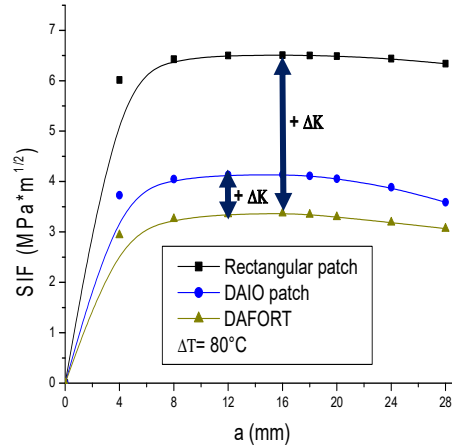


Figure 17. Interaction patch DAFORT- rupture energy gain (+ $\Delta K$ ) in plate

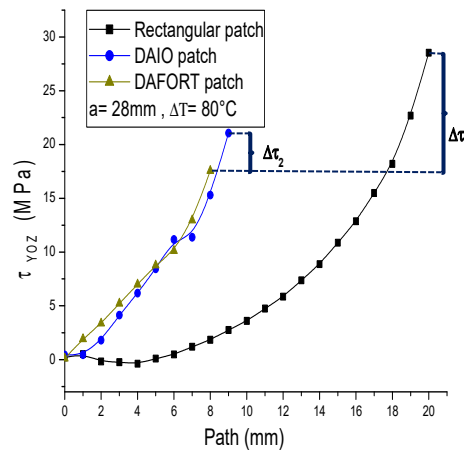


Figure 18. Interaction patch DAFORT-shear stress grain (+ $\Delta\tau$ ) in the adhesive

tangential forces (+ $\Delta\tau$ ) (Fig. 16). Which leads, compared to a DAIO patch, to a more efficient repair in terms of simultaneous gains in rupture energy of the plate (+ $\Delta K$ ), mechanical forces in the adhesive (+ $\Delta\tau$ ) and mass of the composite patch (+ $\Delta m$ ).

For a better illustration of this phenomenon, the impact of a double reduction in the thickness of the DAFO patch, gives a double arrow finally optimized reduced thickness denoted DAFORT ( $ea=0.5$  mm), is explicitly indicated in Fig. 17. The results illustrated in this figure confirm that less rigid patches induce stresses compression due to buckling of low amplitudes, generated by thermal residual stresses, and ensure better stabilization of the hot-repaired crack in terms of fracture energy gain (+ $\Delta K$ ) by a strong drop in the SIF. Compared to the DAOF patch, the repair using a DAFORT patch, with the same covering surface, generates low level shear stresses in the

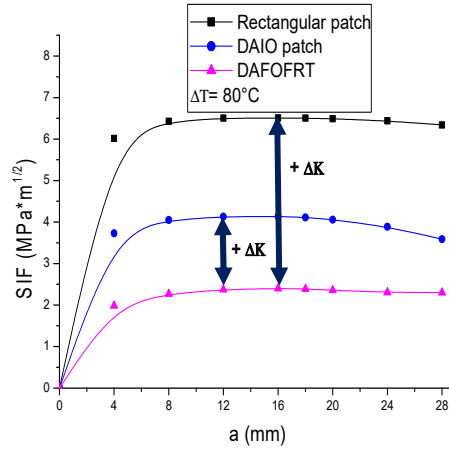


Figure 19. Interaction DAFOFRT patch- rupture energy gain (+ΔK)

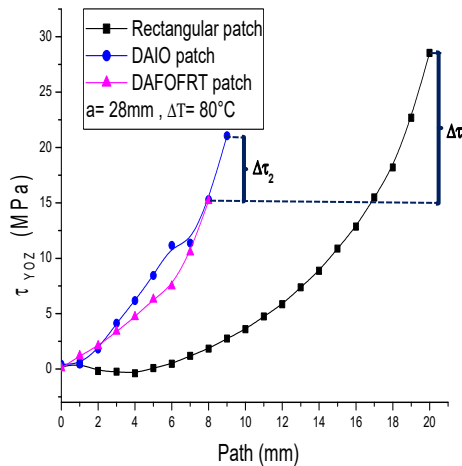


Figure 20. Interaction DAFOFRT- shear stress (+Δτ)

adhesive (Fig. 18), which minimizes the risk of damage to the adhesive joint characterized by a gain in energy (+Δτ). On the other hand, this DAFOFRT patch, doubly thinner than the DAFO patch, presents a mass gain (+Δm) of 50% compared to DAFO and 70% compared to the DA patch.

A more marked reduction, of 50%, in the thickness of the DAFOFRT patch gives rise to a twice-thin patch with thickness of 0.25 mm denoted DAFOFRT (ea=0.25 mm). It should be noted that these repair materials have the same covering area, they differ only in their volume. The second, half as bulky, twice as light in mass, in other words half as rigid, ensures more effective repair of the cracked plate in terms of reducing both the SIF and the crack tips of the plate (Fig. 19), the

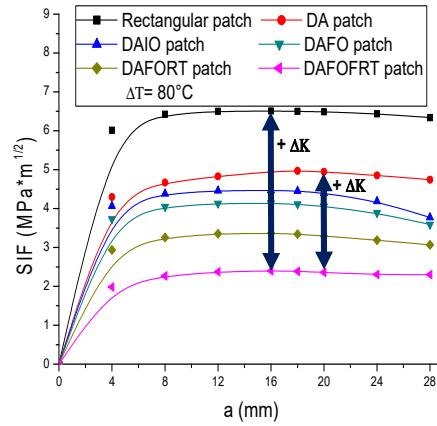


Figure 21. Interaction DAFOFRT patch- rupture energy gain (+ $\Delta K$ ) (All cases)

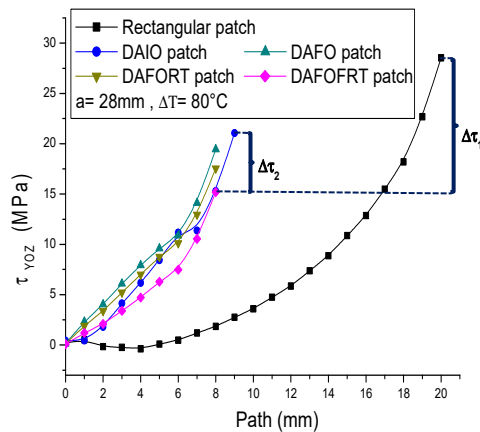


Figure 22. Interaction DAFOFRT- shear stress (+ $\Delta\tau$ ) (All cases)

intensity of the shear stresses in the adhesive (Fig. 20), and the mass of the composite patch, characterized respectively by simultaneous gains in the fracture energy at crack tips (+ $\Delta K$ ), mechanical forces at the adhesive interface (+ $\Delta\tau$ ), and mass of the patch (+ $\Delta m$ ). These gains were evaluated in relation to those resulting from repairs using a patch of rectangular mother shape, double arrow DA, double arrow initially optimized DAIO, double arrow optimized finally with reduced thickness DAFORT, double arrow optimized finally with reduced thickness twice-thin DAFOFRT shown at the figures from Fig. 17 to Fig. 22. Thus, the optimized patch DAFOFRT retained, allowing the simultaneous satisfaction of the three performance criteria (+ $\Delta K$ ), (+ $\Delta\tau$ ), (+ $\Delta m$ ) corresponds to an extremely thin patch of size 0.25 mm. For a mass of 8.58 g measured experimentally using an electronic microbalance, a rectangular mother-shaped patch in unidirectional carbon-epoxy, thickness 02 mm, size 80x40 mm, used as repair material, the masses

of the optimized and developed patches go from 8.58 g (rectangular patch) to 0.429 g (DAFOFRT patch) which corresponds to a mass gain of 95%. For a repaired crack size of 28 mm, this patch development leads to a respective reduction of the SIF in repaired crack tips from  $6.50 \text{ MPa}\cdot\text{m}^{1/2}$  (resulting from the mother shape of the rectangular patch) to  $2.29 \text{ MPa}\cdot\text{m}^{1/2}$  (for a DAFORT patch) and to a drop in the level of shear stresses from 28.45 MPa (rectangular mother patch shape), to 15.19 MPa (DAFOFRT patch). Thus, compared to all other forms of patch, a repair using a DAFOFRT patch simultaneously results in a gain in fracture energy at the crack fronts of the plate ( $+\Delta K$ )= $4.10 \text{ MPa}\cdot\text{m}^{1/2}$ , i.e., a rate ( $+\Delta K/K$ ) of 64%, a gain in mechanical effort in the adhesive joint of ( $+\Delta\tau$ )= $22.58 \text{ MPa}$  i.e., again ( $+\Delta\tau/\tau$ ) of 47% and a gain in mass of the patch composite 8.151 g corresponding to a rate ( $+\Delta m/m$ ) of 95%. In other words, a reduction in the SIF of 63%, a drop in the level of shear stresses in the adhesive joint by 47% and reduction in the mass of the composite patch by 95%. Such a repair is significantly more efficient in terms of stabilization of all three components: plate (fall of the SIF), adhesive (drop of shear stress), patch (drop of the mass of the patch). In addition to these gains, this type of DAFORT patch has a very aesthetic geometry.

For a better illustration of the effectiveness of the patch, hot bonded to the cracked plate of the repair are represented in Fig. 24, Fig. 25 and Fig. 26. For a crack size equal to 28mm, in histogram form the energy gains of rupture of the plate (KI), the gains in shear stresses in the adhesive joint ( $\tau$ ), and the gains in mass of the composite patch (m). These figures clearly show that the DA and optimized double arrow patches, developed from the initially rectangular mother shape, are more effective from a point of view of reducing both the SIF in mode I (KI) in crack front of the plate (Fig. 23), drop in the level of shear stresses in the adhesive joint ( $\tau$ ) (Fig. 25) and reduction in the mass of the composite patch (m) (Fig. 26). The strong drops in these three physical parameters (KI,  $\tau$ , m), closely linked to the three components of the plate-adhesive-patch repair, and illustrated previously as gains ( $+\Delta K$ ,  $+\Delta\tau$ ,  $+\Delta m$ ) and defined as a performance criterion, are significantly more important when the repair is carried out using a DAFOFRT patch. Thus, the repair using a DAFOFRT type patch, where the patch is hot repair to the plate, is incomparably more efficient, in terms of stability of the plate, adhesive and patch.

It should be remembered that all four double arrow patches in Fig. 26, having the same covering area, are only distinguished by their thicknesses. It is clearly illustrated in this figure that thin patches are more effective in terms of fracture energy gain at the repaired crack fronts. Thus, the crack is more stable if the repair is designed using a patch DAIO is slim in size (Fig. 27(b)). This explicitly shows that the rigidity of the patch hot-bonded to the cracked area of the plate is a physical parameter determining the performance of the repair. Thus, the stiffer patches, in other words thicker, generate an elastic buckling of the plate which results in a development of a local parasitic bending of the plate whose forces act as crack opening forces (Fig. 27(a)). The strong instabilities of the crack observed in this case are essentially due to these additional forces. The latter are all the more important as the composite patch has high rigidity, in other words, it is thicker (Fig. 27(a)). For a crack of size 28mm, the DAFOFRT patch, 0.25mm thick as thick as the FM73 adhesive joint, four times less thick than that of the DAIO patch, presents, compared to the latter, both an energy gain rupture ( $+\Delta K/K$ ) of 40%, a gain in shear forces of 27% and a mass gain of 87% (Fig. 16). And compared to a mother form of rectangular patch a  $+\Delta K/K$  of 64% (Fig. 23),  $+\Delta\tau/\tau$  of 47% (Fig. 24), and  $+\Delta m/m$  of 95% (Fig. 25). The gain in fracture energy of the plate ( $+\Delta K/K$ ) is due to the strong interaction between the singular parts of the double arrow patch DAFORT and the crack fronts, on the one hand, and between the interaction between the low rigidity of the patch and the level of parasitic normal stresses generated by the buckling of the

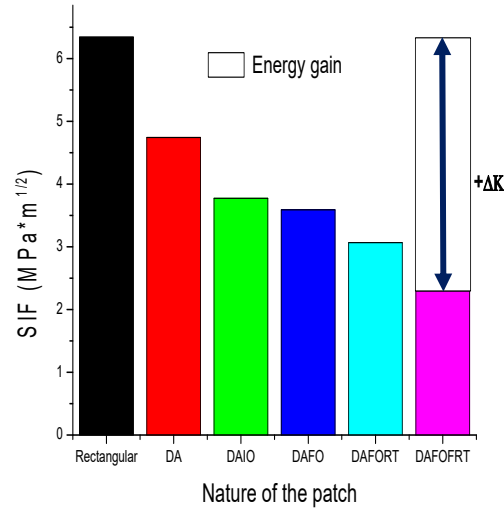
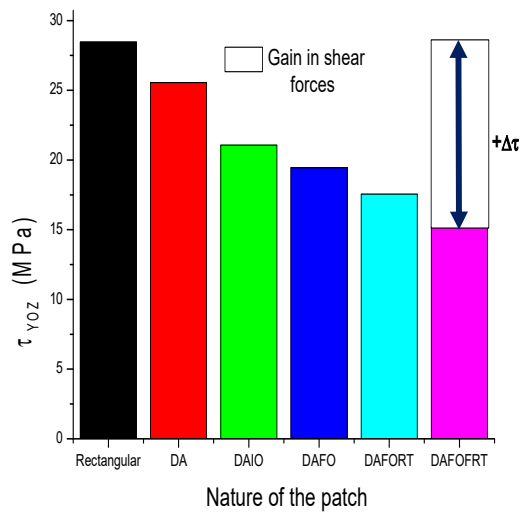


Figure 23. Interaction patch shape - rupture energy gain in plate (KI)

Figure 24. Interaction patch shape - Shear stresses in the adhesive ( $\tau$ )

cracked plate. The considerable drop, of eight times, in the thickness of the patch compared to the rectangular patch, otherwise an eight-fold reduction in the rigidity of the patch, is responsible for the improvement in the gain in shear forces in the adhesive joint ( $+\Delta\tau/\tau$ ). The successive reduction of this thickness is at the origin of the considerable gain in mass of the composite patch ( $+\Delta m/m$ ). The originality of this study lies in the simultaneous development of these parameters

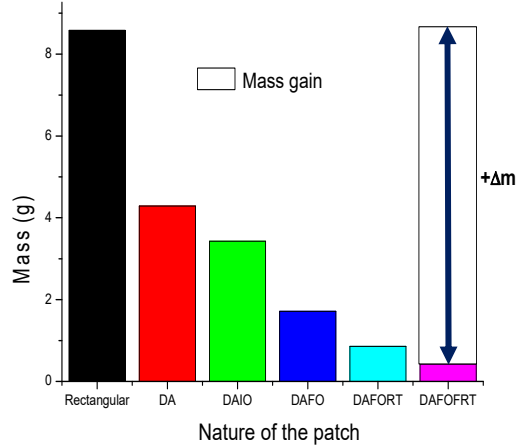


Figure 25. Interaction patch shape-mass gain of the composite patch (m)

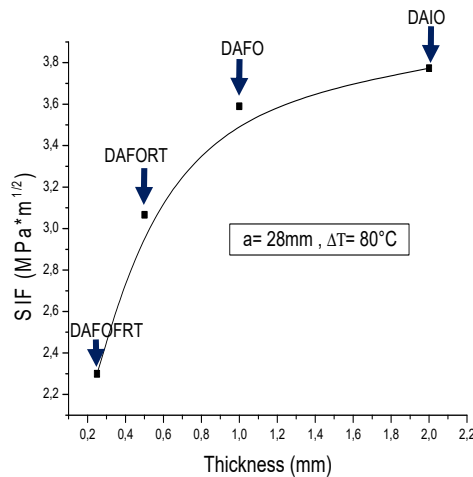


Figure 26. Interaction stiffness of the optimized patch-rupture energy gains (KI)

( $+\Delta K/K$ ), ( $+\Delta\tau/\tau$ ), ( $+\Delta m/m$ ) characteristics of the repair performance. This shows that the patch in the ultimately optimized double arrow shape, DAFOFRT, ensures that the cracked and repaired plate has good mechanical strength in service by both minimizing the risk of crack propagation (by gaining energy from rupture of the plate  $+\Delta K/K$ ), the risk of rupture of the adhesive (by a gain in shear forces in the adhesive  $+\Delta\tau/\tau$ ), and the mass of the patch (by a gain in mass  $+\Delta m/m$ ). This behavior leads to a mechanical stabilization of the three elements of the repair: plate-adhesive-patch of the repair. Our results exclusively show that the hot bonding of this type of DAFOFRT patch to the cracked plate is significantly more efficient in terms of simultaneous gains in these three physical parameters.

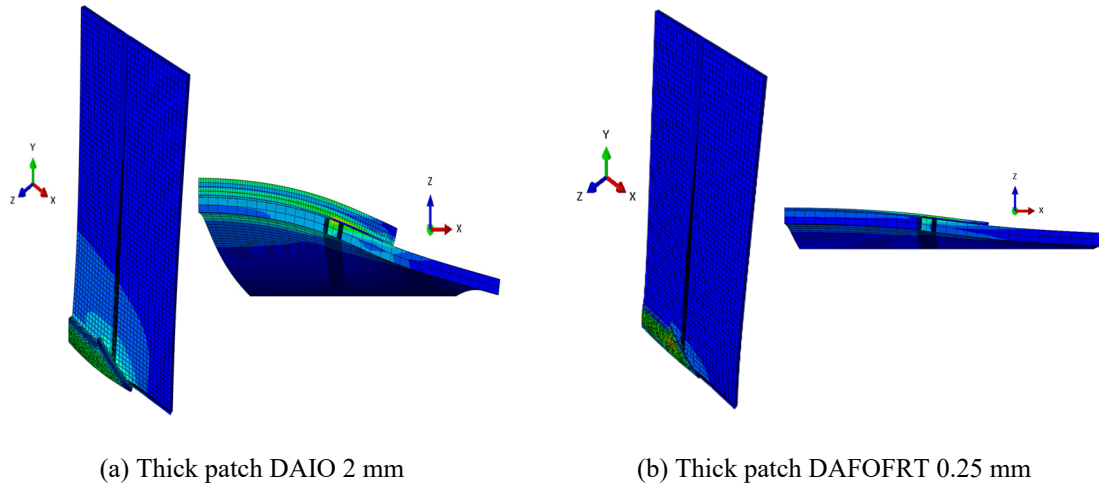


Figure 27. Patch stiffness-plate buckling interaction

On the other hand, thin patches significantly improve the aerodynamic resistance of the repair, and minimize peel stresses and shear stresses in the adhesive and their interaction effect. This behavior results in an increase in service life and repair performance.

#### 4. Conclusions

This work, based on hot bonding of the composite patch to the cracked area of the Al2024T3 plate, has allowed for the first time the development of three characteristic criteria of the repair performance ( $+\Delta K/K$ ), ( $+\Delta\tau/\tau$ ), ( $+\Delta m/m$ ), and this whatever the nature of the cold or hot bonding. These criteria, closely linked to the three components, damaged plate-adhesive-patch, show that the hot patch-plate junction doesn't affect the repair performance in terms of simultaneous gains in plate fracture energy, shear stress in the adhesive and mass of the patch. This can only be achieved by a reduction in both the fracture energy at the crack fronts of the plate ( $\Delta K$ ), the shear stresses in the adhesive joint  $\Delta\tau$ , and the mass of the patch. This study highlighted that this condition necessary for the effectiveness of the repair can only be satisfied by optimizing the shape of the composite patch. The impact of six shapes, resulting from an initially rectangular, elliptical, orthogonal, star, H, double arrow and butterfly shape, on the stabilization of the crack (reduction of the SIF) and that of the patch (reduction of the mass of the composite patch). It emerges from this study that, contrary to all the analyzed geometries of the patch, the repair performance using a double arrow shaped patch DA, in terms of fracture energy gains  $\Delta K/K$ , shear stress gain in the adhesive  $\Delta\tau/\tau$ , and mass gain  $\Delta m/m$ , is more efficient. This efficiency is significantly improved by a reduction in the dimensional parameters of the DA patch, in a DA patch (DAIO) with a 20% lower coverage area. The repair using the DAIO patch is characterized simultaneously by strong gains in the crack propagation energy of the plate ( $+\Delta K/K$ ), shear stresses in the adhesive ( $+\Delta\tau/\tau$ ), and mass of the patch ( $+\Delta m/m$ ). These gains are distinctly more consistent when the repair is performed using a thin DAIO patch.

This study shows that hot bonding a DAFOFRT patch eight times thinner (thickness deducted from 88%) than the DA, and mass gain ( $+\Delta m/m=95\%$ ), generates low normal residual stresses which in no way affect the efficiency of hot bonding the patch to the plate. On the other hand, thin patches improve the aerodynamic resistance of the repair and reduce peel stresses and shear stresses and minimize their interaction effect often responsible for the damage of the repair.

## References

1. Kim, S., Ha, J., Yoon, S., Kim, M. (2020). A study on mechanical properties after bonded repair of sandwich composite materials. *Journal of Modern Physics Letters B*, 34(7-9), 2040033. <https://doi.org/10.1142/S0217984920400333>.
2. Bezzerrouki, M., Bachir-Bouiadjra, B., Ouinas, D. (2008). Stress intensity factors for cracks repaired with a single composite patch having two adhesive bands and a double symmetric patch in aircraft structures. *Computational Materials Science*, 44, 542–546. <https://doi.org/10.1016/j.commatsci.2008.04.029>.
3. Belhoucine, A., Madani, K. (2022). Effect of composite patch beveling on stress reduction in damaged 2024-T3 aluminum structures repaired by composite and hybrid patches. *Structural Engineering and Mechanics*, 82(1), 17-30. <https://doi.org/10.12989/sem.2022.82.1.017>.
4. Zagane, M.E.S., Moulgada, A., Sahli, A., Baltach, A., Benouis, A. (2023). Study of fracture behavior of different structures using the extended finite element method (XFEM). *Advanced Materials Research*, 12(4), 273-286. <https://doi.org/10.12989/amr.2023.12.4.273>.
5. Allem, A., Salem, M., Talbi, S., Sahli, A. (2023). Numerical study of mechanical behavior of repaired inclined cracks under combined shear loading in aluminum 2024-T3. *Journal of the Serbian Society for Computational Mechanics*, 17(2), 38-54. <https://doi.org/10.24874/jsssem.2023.17.02.04>.
6. Ouinas, D., Hebbar, A., Bachir-Bouiadjra, B., Belhouari, M., Serier, B. (2009). Numerical analysis of stress intensity factors for repaired cracks using a bonded composite semicircular patch. *Composites Part B: Engineering*, 40(8), 804-810. <https://doi.org/10.1016/j.compositesb.2009.06.002>.
7. Mhamdia, R., Serier, B., Bachir-Bouiadjra, B., Belhouari, M. (2012). Numerical analysis of patch shape effects on the performance of bonded composite repairs in aircraft structures. *Composites Part B: Engineering*, 43(2), 391-397. <https://doi.org/10.1016/j.compositesb.2011.08.047>.
8. Deheeger, A., Badulescu, C., Mathias, J.D., Grédiac, M. (2009). Experimental study of thermal stresses in a bonded joint. *Journal of Physics: Conference Series*, 181, Article 012041. <https://doi.org/10.1088/1742-6596/181/1/012041>.
9. Azzouz, A., Mhamdia, R., Kaddouri, K., Benarbia, D. (2021). Numerical analysis of bonded composite shape effects under thermal loading in aircraft structures. *Advanced Materials Research*, 1167, 1-11. <https://doi.org/10.4028/www.scientific.net/AMR.1167.1>.
10. Albedah, A., Mhamdia, R., Benyahia, F., Bachir-Bouiadjra, B., Serier, B. (2014). Analysis of thermal residual stress distribution in circular and elliptical bonded composite repairs of cracked structures. *Key Engineering Materials*, 577-578, 681-684. <https://doi.org/10.4028/www.scientific.net/KEM.577-578.681>.
11. Aminallah, L., Benhamena, A., Aid, A., Bachir-Bouiadjra, B., Serier, B., Benseddiq, N. (2012). Finite element analysis of the effect of thermal residual stresses on the performance of bonded composite repairs in aircraft structures. *Proceedings of the 14th International Materials Symposium (IMSP 2012)*.
12. Kondratiev, A., Pistek, V., Smovziuk, L., Shevtsova, M., Fomina, A., Kucera, P., Prokop, A. (2021). Effects of the temperature–time regime of curing of composite patch on repair process efficiency. *Polymers*, 13, 4342. <https://doi.org/10.3390/polym13244342>.
13. Kumaran, M., Senthilkumar, V., Justus Panicke, C.T., Shishir, R. (2021). Investigating residual stress in additive manufacturing repair by directed energy deposition on SS316L substrate. *Materials Today: Proceedings*, 47(14), 4475-4478. <https://doi.org/10.1016/j.matpr.2021.05.319>.

14. Ibrahim, C.N., Fari-Bouanani, M., Bachir-Bouiadjra, B., Serier, B. (2016). Analysis of adhesive damage between composite and metallic adherends applied to aircraft structure repair. *Advanced Materials Research*, 5(1), 11-20. <https://doi.org/10.12989/amr.2016.5.1.011>.
15. Ibrahim, N.C., Boualem, S., Belaid, M. (2018). Analysis of crack interaction effects in aeronautical structures repaired by composite patches. *Frattura ed Integrità Strutturale*, 12(46), 140-149. <https://doi.org/10.3221/IGF-ESIS.46.14>.
16. Azzeddine, N., Benkheira, A., Fekih, S.M., Belhouari, M. (2020). Numerical study of bonded composite patch repair in damaged laminate composites. *Advances in Aircraft and Spacecraft Science*, 7(2), 151-168. <https://doi.org/10.12989/aas.2020.7.2.151>.
17. Moallem, M.D., Barzegar, M., Abedian, A., Kordkheili, S.H. (2021). Effects of fiber volume fraction on fatigue behavior of bonded composite patch repairs in damaged aluminum plates. *Journal of Reinforced Plastics and Composites*, 40(1-2), 29-40. <https://doi.org/10.1177/0731684420941150>.
18. Baker, A.A., Nezhad, H.Y. (2021). Adhesively bonded repairs to highly loaded structures. (Ed., R.D. Adams), *Adhesive bonding*, 2nd Ed., 437-497. Woodhead Publishing. <https://doi.org/10.1016/B978-0-12-819954-1.00022-8>.
19. Mohammadi, S. (2022). The effect of disbond on efficiency and durability of composite patch repairs under mode I and mixed-mode loading. *Polymers and Polymer Composites*, 30. <https://doi.org/10.1177/09673911211062759>.
20. Aminallah, S., Fekih, S.M., Sahli, A. (2023). Optimization of scarf patch stacking sequences using design of experiments. *Advances in Aircraft and Spacecraft Science*, 10(4), 335-346. <https://doi.org/10.12989/aas.2023.10.4.335>.
21. Xing, R., Wang, F., Yang, Y., Li, G. (2024). Optimization of composite repair patch shape based on strength analysis. *Applied Sciences*, 14, 4397. <https://doi.org/10.3390/app14114397>.
22. Bellali, M.A., Mokhtari, M., Benzaama, H., Fekirini, H., Serier, B., Madani, K. (2020). Using CZM and XFEM to predict damage in aluminum notched plates reinforced with composite patches. *Mechanics of Materials and Structures*, 15(2), 185-200. <https://doi.org/10.2140/jomms.2020.15.185>.
23. Coudor, P. (2009). Analyse fine du mécanisme d'interaction dans les structures souples assemblées par collage (Doctoral dissertation, Université Blaise Pascal). <https://tel.archives-ouvertes.fr/tel-00725912>.
24. Barsoum, R.S. (1976). On the use of isoparametric finite elements in linear fracture mechanics. *International Journal for Numerical Methods in Engineering*, 10(1), 25-37. <https://doi.org/10.1002/nme.1620100103>.
25. Hattali, L. (2009). Caractérisation et modélisation thermomécaniques des assemblages métal-céramique élaborés par thermocompression (Doctoral dissertation, École Centrale de Lyon).
26. Cognard, J. (2004). *Science et technologie du collage*, 1st Ed., Presses polytechniques et universitaires romandes.
27. Zaoui, B., Baghdadi, M., Mechab, B., Serier, B., Belhouari, M. (2019). Experimental and numerical prediction of weakened zones in ceramic-metal bonded joints. *Advanced Materials Research*, 8(4), 295-311. <https://doi.org/10.12989/amr.2019.8.4.295>.
28. Kaddouri, K., Ouinas, D., Bachir-Bouiadjra, B. (2008). Finite element analysis of octagonal bonded composite repairs in aircraft structures. *Computational Materials Science*, 43(4), 1109-1115. <https://doi.org/10.1016/j.commatsci.2008.03.003>.
29. Bachir-Bouiadjra, B., Fari-Bouanani, M., Albedah, A., Benyahia, F., Es-Saheb, M. (2011). Comparison between rectangular and trapezoidal bonded composite repairs in aircraft structures: a numerical analysis. *Materials & Design*, 32(6), 3161-3166. <https://doi.org/10.1016/j.matdes.2011.02.053>.
30. Ramji, M., Srilashmi, R., Bhanu Prakash, M. (2012). Optimization of patch shape for bonded composite repair using finite element methods. *Composites Part B: Engineering*, 45(1), 710-720. <https://doi.org/10.1016/j.compositesb.2012.07.049>.
31. Li, C., Zhao, Q., Yuan, J., Hou, Y., Tie, Y. (2019). Simulation and experimental study on patch shape effects in adhesive repair of composite structures. *Composites Science and Technology*, 53, 4125-4135. <https://doi.org/10.1177/0021998319853033>.
32. Mohammadi, S., Yousefi, M., Khazaei, M. (2020). A review of composite patch repairs and key

- parameters affecting efficiency and durability. *Journal of Reinforced Plastics and Composites*, 40, 1-13. <https://doi.org/10.1177/0731684420941602>.
33. Caliskan, U., Ekici, R., Yildiz-Bayazit, A., Apalak, M.K. (2021). Numerical modeling of composite patch repair of notched aluminum plates under impact loading. *Proceedings of the Institution of Mechanical Engineers, Part L: Journal of Materials: Design and Applications*, 235(5), 958-973. <https://doi.org/10.1177/1464420720983375>.
  34. Donadio, F., Papa, I., Viscusi, A. (2024). Experimental analysis of repaired CFRP using innovative hot bonding technology. *International Journal of Advanced Manufacturing Technology*, 132, 3507-3518. <https://doi.org/10.1007/s00170-024-13592-x>.